European Polymer Journal 44 (2008) 3931–3940

Contents lists available at ScienceDirect

European Polymer Journal

journal homepage: www.elsevier.com/locate/europolj

Macromolecular Nanotechnology

Microscopic morphology of blends between a new "all-acrylate" radial block copolymer and a rosin ester resin for pressure sensitive adhesives

M. Jeusette [a,*], S. Peeterbroeck [b], F. Simal [c,1], D. Cossement [d], P. Roose [c], Ph. Leclère [a], Ph. Dubois [b], M. Hecq [d], R. Lazzaroni [a]

[a] Service de Chimie des Matériaux Nouveaux, Centre d'Innovation et de Recherche en Matériaux Polymères (CIRMAP), Université de Mons-Hainaut, Place du Parc, 20, B-7000 Mons, Belgium
[b] Service des Matériaux Polymères et Composites, Centre d'Innovation et de Recherche en Matériaux Polymères (CIRMAP), Université de Mons-Hainaut, Place du Parc, 20, B-7000 Mons, Belgium
[c] Cytec, Surface Specialties S.A., Anderlechtstraat 33, B-1620 Drogenbos, Belgium
[d] Laboratoire de Chimie Inorganique et Analytique (Materia-Nova center), Université de Mons-Hainaut, Place du Parc, 20, B-7000 Mons, Belgium

ARTICLE INFO

Article history:
Received 28 April 2008
Received in revised form 2 September 2008
Accepted 3 September 2008
Available online 11 September 2008

Keywords:
Radial copolymers
Rosin resin
Adhesives
Tackifying resin
AFM
Gordon-Taylor

ABSTRACT

With the goal of developing new pressure sensitive adhesive systems, the miscibility and the phase morphology of blends between novel symmetric four-arm star "all-acrylate" block copolymers synthesized by atom transfer radical polymerization (ATRP) and a rosin ester resin tackifier was studied with a combined differential scanning calorimetry (DSC) and atomic force microscopy (AFM) approach. Copolymer–resin compositions with increasing resin content in the blend were studied. The DSC results show good miscibility for compositions lower than 60 wt%, with a single glass transition at a temperature between those of the two pure compounds. The AFM results indicate that the initial two-phase morphology typical of the block copolymer matrix is preserved up to 60 wt% of resin. Above that value, a third phase, attributed to aggregates of the pure resin, is observed. Upon ageing, the homogeneous systems (e.g., blends with 40 wt% of resin) undergo a slow migration of the tackifying resin towards the surface of the sample, which can be understood in terms of surface free energy considerations. This eventually leads to the formation of a layer of pure resin at the surface.

1. Introduction

Pressure sensitive adhesives (PSAs) are of particular interest because of their inherent tackiness, which allows them to quickly wet and adhere under a light pressure on a broad variety of substrates [1]. The first generation of PSAs was elaborated by blending natural rubbers with low-molecular-weight, miscible additives in approximately equal proportions [2]. Nowadays, most PSA's are synthetic, viscoelastic materials based on styrenic block copolymers (SBC), acrylic copolymers or silicone elastomers [3]. Among these, SBC's still represent a large portion of the materials used in a wide variety of PSA applications. Their particular morphology, where thermoplastic nanoscale domains dispersed in a rubbery matrix act as physical crosslinks, provides high elasticity and gives these PSA's superior resistance to creep.

However, as rubbery materials, SBC's cannot be used as such for PSA. Consequently, it is necessary to formulate them with additives like tackifying resins [4]. Tackifying resins are amorphous, oligomeric materials such as rosins,

* Corresponding author. Tel.: +32 65373865; fax: +32 65373861.
E-mail address: melanie.jeusette@umh.ac.be (M. Jeusette).
[1] Present address: Hexion Specialty Chemicals S.A., 1, Avenue Jean Monnet, 1348 Ottignies Louvain-la-Neuve, Belgium.

0014-3057/$ - see front matter © 2008 Elsevier Ltd. All rights reserved.
doi:10.1016/j.eurpolymj.2008.09.003

terpene resins, or hydrocarbon resins [5]. Typically, the addition of a tackifier provides a lower modulus so that the polymer can flow and wet the substrate to form an adhesive bond, providing the viscoelasticity required for the finished adhesive. In some cases, the polar sites on the tackifier may also interact with the surface of the substrate to help forming an effective bond. Those resins are usually chosen to be selectively compatible either with the elastomer part or the thermoplastic part of the copolymer. In general, tackifying resins compatible with both constituents of the copolymer should be avoided as they tend to weaken the PSA properties of the product [6]. Carefully chosen resins can lead to improvement of tack and adhesion on specific substrates. In terms of the copolymer base, the development of star/radial (co)polymers has received increasing interest, due to their better mechanical properties as compared to their linear counterparts [7].

Although the recent developments in SBC's have allowed the improvement of many specific properties (improvement of tack, adhesion on polar substrates, resistance to higher temperatures (Shear Adhesion Failure Temperature test and ageing and UV resistance), the development of their full acrylic countertypes has always been a long–sought goal. Acrylate block copolymers having the ability to phase-separate on the nanoscale, are expected to perform better in terms of durability, resistance to photodegradation, heat resistance and tack as compared to SBC's [8]. Although further formulation of the base may not be a pre requisiste due to their inherent and adjustable adhesion power, the addition of a tackifier can also be considered to optimize their dissipative properties by adjusting the glass transition temperature (T_g) and to further modify their adhesion properties by inducing specific interactions [9,10].

Because the miscibility between the polymer and the tackifier is expected to affect the phase structure in the solid-state, the mechanical properties and the practical performance of the PSA [9], it is critical to study the compatibility between the components (copolymer and additive) of a given formulation.

In order to determine the solid-state phase structure of a tackified acrylic block copolymer, tapping mode atomic force microscopy (TMAFM) has been used in this study, since it is a powerful technique for the observation of phase-separated morphologies at the nanoscale. Moreover, in the case of "all-acrylate" block copolymers, the very low electronic contrast between the constitutive blocks is a major problem for the observation of morphologies by transmission electron microscopy (TEM) and small angle X-ray scattering (SAXS). Therefore, AFM appears as the most suitable tool for the direct observation of phase separation in this class of block copolymers [11] and their blends.

In this study, the miscibility and the phase morphology of blends between a poly((2-EHA-*co*-MA)-MMA)$_4$ "all-acrylate" star copolymer and a rosin ester resin tackifier (Scheme 1) were studied by differential scanning calorimetry (DSC) and TMAFM. Different copolymer–resin compositions with increasing resin content in the blend were studied, with particular interest focused on the compatibility between the tackifier and the elastomer part of the copolymer. In these systems, a good miscibility of the tackifying resin with the elastomer part is an important premise to produce adhesives with good tack.

Ageing is another factor that may result in a detrimental effect on the PSA properties of a given composition. Any modification in time of the miscibility between the different components of the copolymer/resin PSA composition can lead to a modification of some PSA's properties. Especially for acrylic PSA's, the use of a tackifying resin decreases the resistance upon ageing of the copolymer/resin PSA mixture. Indeed, the PSA composition can undergo a slow phase separation and surface segregation [1]. In order to better understand the effect of ageing on the acrylic copolymer–rosin systems, we have also studied by AFM the evolution of the phase morphology of a blend with a resin content of 40 wt%.

2. Experimental

2.1. Materials

The "all-acrylate" copolymer studied here is a radial block copolymer denoted as $(A–B)_n$ where A and B represent an elastomer segment (A = P(2EHA-*co*-MA) = *poly*(2-ethylhexyl acrylate-*co*-methyl acrylate)) and a thermoplastic segment (B = PMMA = *poly*(methyl methacrylate)), respectively. In the present notation, the index n relates to the structural arrangement, e.g., $n = 4$ stands for a four-arm radial block structure. The synthesis of this

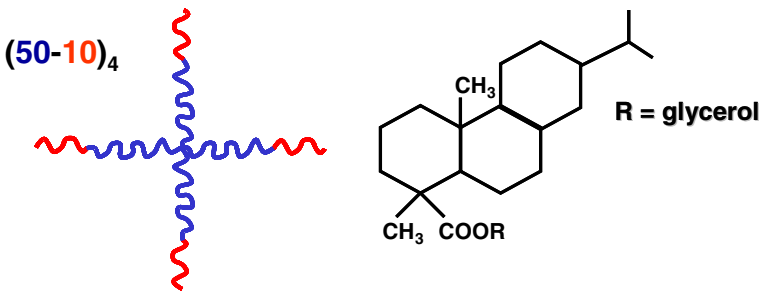

Scheme 1. Sketch of (left) the "all-acrylate" star copolymer. This star copolymer is denoted as $(A–B)_4$ where A and B represent the elastomer segment (A = P(2EHA-*co*-MA) = *poly*(2-ethylhexyl acrylate-*co*-methyl acrylate)) and the thermoplastic segment (B = PMMA = *poly*(methyl methacrylate)), respectively. (right) the tackifying resin, which is a hydrogenated rosin glycerol ester.

copolymer has been described previously [12]; its main characteristics are listed in Table 1. The tackifying resin is a commercially available hydrogenated rosin resin, esterified by glycerol (Foral 85-E, Eastman). The properties of this resin are listed in Table 2.

2.2. DSC analysis

The samples were prepared by casting a copolymer–resin solution in toluene, in a porcelain dish covered with a silicone paper. Slow solvent evaporation was achieved under a saturated toluene atmosphere for 24 h; the films were then dried at room temperature for one week. DSC thermograms were measured with a DSC Q200 (TA Instruments) at a linear heating rate of 10 °C/min. The sample mass was ≈10 mg. During a first scan, the samples were heated to 150 °C and cooled at 10 °C/min to −75 °C; during the second scan, the samples were heated again to 150 °C. The T_g-values reported here were obtained from the second scan.

2.3. AFM analysis

Thin films of the copolymers were prepared by solvent casting from toluene solutions on freshly-cleaved mica substrates. These films were evaporated under a saturated atmosphere of toluene for 48 h, and then dried in ambient atmosphere for 24 h. The thickness of the films was measured by ellipsometry using the following values for refractive indexes: 1.45 for the radial block copolymer; 1.50 for the hydrogenated rosin resin and 1.58 for the mica substrate. The typical thickness (i.e., 700 ± 200 nm) was chosen in order to make sure that: (i) the film surface is smooth (thicker films tend to be rougher and the topographic contrast can perturb the phase image) and (ii) the morphology is not affected by specific interactions with the substrate, as is often the case when the thickness is of the same order of magnitude as the microdomain size [13]. Since toluene is a good solvent for the investigated (meth)acrylate copolymers, selective precipitation was not expected to influence the morphology. The samples were first analyzed after complete evaporation of the solvent at room temperature.

The AFM measurements were performed in "tapping mode" (TMAFM). In this mode, the cantilever holding the probe tip oscillates close to the resonance frequency above the sample surface, so that the tip is in short-time contact with the surface at the lower end of the oscillation. The phase of the oscillating tip is very sensitive to the nature of the interaction with the surface. It has been shown that the phase lag can be directly related to the elastic modulus of the material when the amplitude is only slightly damped upon contact with the surface [14]. Therefore, simultaneous recording of the phase and the height images provides a map of the local mechanical properties and allows phase-separated microdomains to be observed. All the AFM images were recorded with a Nanoscope IIIa microscope operated at room temperature in air using commercial cantilevers from Olympus Corporation. The cantilever characteristics are the following:

- Silicon cantilever with aluminium reflex coating on the cantilever back side.
- Resonance frequency of 70 kHz with a spring constant of 1 to 5 Nm^{-1}.
- Tip radius <10 nm.
- The tip on the cantilever is a tetrahedral tip with symmetrical side angle; the tip is located exactly at the cantilever end.

Different areas ($3 \times 3\ \mu m^2$) of $1.5 \times 1.5\ cm^2$ samples were inspected with scanning times of *ca.* 8 min. The images were digitally sampled at the maximum number of pixels (512) in each direction and the Nanoscope image processing software was used for image analysis. Unless otherwise stated, image treatment was limited to a "flattening" operation, whereby a first-order surface, representing height variations related to a possible tilt of the sample, is subtracted from the original image. In order to compare the different copolymer–resin blends, all samples were imaged with the same tip, with the same free amplitude and scanning parameters.

2.4. ToF-SIMS analysis

ToF-SIMS measurements were carried out on an ION-TOF TOFSIMS IV spectrometer using a pulsed Ar^+ argon primary ion beam (10 keV, I_{target} = 1 pA) rastered for 100 s over a $300 \times 300\ \mu m^2$ area with an incidence angle of 45°. A compensation charge gun was used due to the electrically insulating nature of the samples. This experimental set-up ensures "static SIMS" conditions for all experiments. Both positive and negative secondary ion mass spectra were recorded.

Table 1
Main characteristics of the radial block copolymer

Mn (kg mol^{-1})	223000
M_w/M_n	5
T_g of the elastomer part by DSC (°C)	−39
T_g of the thermoplastic part by DSC (°C)	98
Average vol. % PMMA	16

Table 2
Main characteristics of the tackifying resin

MM (g/mol)	∼950
ρ (g/cm^3)	1.06
T_g by DSC (°C)	37
Softening point (°C)	∼80

3. Results and discussion

3.1. Miscibility between the radial block copolymer and the tackifying resin

Thermal analysis by DSC is a recognized method to examine the miscibility between the components in a blend. The phase behavior can be related to the number of glass transitions detected in the thermogram. The presence of multiple glass transitions is a clear signature of phase separation, which reflects the immiscibility of the

components. In contrast, a single glass transition at an intermediate temperature between those of the pure components is an indication of miscibility.

As mentioned in the introduction, we are interested more particularly in the compatibility of the tackifier with the elastomer part of the copolymer. Fig. 1 shows the DSC thermograms for increasing amounts of tackifying resin in the copolymer–resin blend. All thermograms show a single glass transition located between the glass transition temperature (T_g) of the P(2EHA-*co*-MA) elastomer part of the copolymer (≈−40 °C) and that of the rosin ester resin (≈37 °C). The glass transition of the thermoplastic phase around 100 °C is not clearly visible due to the small contribution of this component to the system (16 vol.% PMMA in the copolymer). Independent experiments showed that the resin is not miscible with PMMA. DSC thermograms (not presented here) recorded on several blends of a pure PMMA homopolymer, with a molar mass equivalent to that of the hard segment of the block copolymer, and the tackifying resin have revealed that there were two distinct glass transitions with T_g-values close to the values of the pure compounds. Hence, it is inferred that there is no miscibility between PMMA and the tackifying resin. The DSC results indicate that only the elastomer part of the copolymer is miscible with the tackifier in the solid-state. We also observe a gradual increase of the T_g for increasing resin contents, as expected from the highest value of T_g for the pure resin.

The phenomenological expression of Gordon–Taylor is often used to describe the relationship between the T_g of a blend and its composition.

$$T_g = (w_1 T_{g1} + k w_2 T_{g2})/(w_1 + k w_2)$$

where T_g, T_{g1} and T_{g2} are the glass transition temperatures of the blend, the acrylic polymer (1), and the tackifier resin (2), respectively; w_1 and w_2 are the weight fractions of the components; and k is the adjusting parameter related to the degree of curvature of the T_g-composition diagram. This curvature is generally believed to be large in polymer/polymer blends with strong interactions between the different polymer segments [9,15]. Several authors [9,16] have suggested that the k value gives a qualitative measure of the degree of interaction between components in the blend, a higher value of k being the signature of a higher degree of interaction.

The dependence of the glass transition temperature upon resin content is plotted in Fig. 2. The experimental T_g-values (*cf.* Fig. 1) are shown by the cross symbols and reveal a monotonous increase towards the value of the pure tackifying resin for contents lower than 70 wt%. Beyond this point, the measured T_g-values deviate from the continuous trend. A fit of the GT-equation to the experimental data, disregarding the deviating values, is represented by the full line. After adjustment, the value of $k = 0.55 \pm 0.07$ suggests a modest affinity between the resin and the elastomer matrix formed by the radial copolymer.

For a resin content higher than 70 w%, the experimental T_g-values indicate a loss of miscibility in the copolymer–resin system where the elastomer matrix becomes saturated. However, it is noticed that there is no clear evidence of a second glass transition (corresponding to the pure resin) in the thermograms. If any, this transition is expected to be small and hardly detectable. A similar observation was reported by Kim and Mizumachi [17] on a mixture between an acrylic copolymer and an esterified rosin; rheological measurements indicate that for resin contents higher than 50 wt%, a second glass transition appears, whereas the DSC results still showed a single glass transition.

In this study, TMAFM was used to investigate the phase behavior of the radial block copolymer with increasing amounts of rosin ester. AFM can provide information on the miscibility between the copolymer and the resin. Indeed, the immiscibility between the elastomer part of the copolymer and the rosin ester resin would be marked by the appearance of a third phase (besides the elastomer phase and thermoplastic phase of the copolymer) or as a resin layer covering the copolymer layer. For block

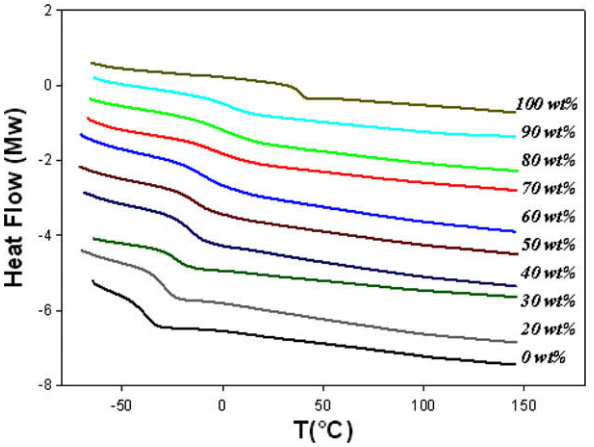

Fig. 1. DSC thermograms for different blends between the copolymer and the tackifying resin, for increasing amounts of resin (in wt%).

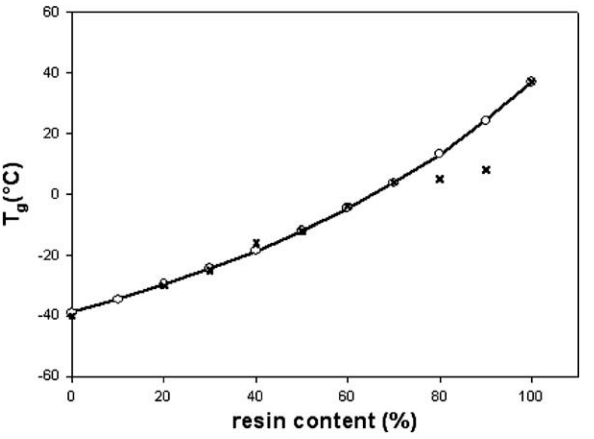

Fig. 2. Plot of T_g for blends of the copolymer and the tackifying resin as a function of resin content (wt%). The cross symbols stand for the experimental data. The open symbols and the full line result from an non-linear regression of the Gordon–Taylor expression to the experimental T_g- values at resin contents lower than 70 wt%.

copolymers, the presence of a phase-separated morphology can be evidenced from the phase images obtained in TMAFM. Here, no attempt was undertaken to analyze the absolute values of the phase signal; the vertical greyscale, and the contrast of the phase images are chosen in order to produce the best contrast and better distinguish the different components. From the AFM images, the periodicity (the average center-to-center distance between thermoplastic domains), and their average diameter can then be determined.

Fig. 3a shows a typical AFM phase image for the pure acrylate radial copolymer [12]. The film surface clearly shows an assembly of bright dots, i.e., areas where the phase lag is higher, dispersed in a dark matrix, where the phase lag is lower. This is a clear signature of microphase separation. Since the phase shift is related to the Young's modulus [14], the bright spots can be assigned to PMMA, which is harder than the elastomer segment constituted of P(2EHA-*co*-MA). From the power spectrum analysis of the images, the average center-to-center distance between the dots is estimated to be 60 ± 5 nm. As indicated by the two-dimensional Fourier transform of the image (inset Fig. 3a), the PMMA spheres are regularly spaced but there is no long-range ordered structure. As reported previously [18], long-range order is observed in films of block copolymers only if the solution is evaporated very slowly and if annealing is carried out for several days or weeks. In this work, the samples were prepared by casting the pure copolymer (or the different copolymer–resin blends) from toluene solutions. The solvent was evaporated in such conditions that phase separation clearly occurs without the appearance of long-range order.

Fig. 3b and c show phase images for blends of the acrylate radial copolymer and the rosin ester resin where the resin content is 40 and 60 wt%, respectively. For these systems, the film surface exhibits a morphology which is similar to that of the copolymer without resin (i.e., hard spheres in a soft matrix, Fig. 3a). This confirms that the elastomer part of the copolymer and the tackifying resin are miscible in this composition range.

In order to highlight the effect of the increase of the resin content on the spatial distribution of the PMMA spheres, we analyzed the phase images in terms of the occupancy ratio at the surface, i.e., for a given image size, we have determined the area occupied by the PMMA spheres at the surface of the blends with an image analysis routine [19]. Fig. 4 shows the evolution of the area occupied by the PMMA spheres on the surface as a function of the resin content. For all the blends, the average diameter of the spheres remains constant around 26 nm, which is consistent with the fact that the resin does not incorporate into the PMMA domains. In the range between 20 and 60 wt% of resin content, the number density of PMMA spheres on the surface decreases for increasing resin contents, consistent with the increase of the average distance between the bright spheres that can be seen on the images. This result confirms the incorporation of the rosin ester resin in the elastomer matrix and the miscibility between those two partners.

For resin contents higher than 60 wt% (here 70, 80 and 90 wt%), we can observe on the AFM phase images the presence of bright, non spherical defects at the surface of the film (marked by arrows in Fig. 5). The size and the

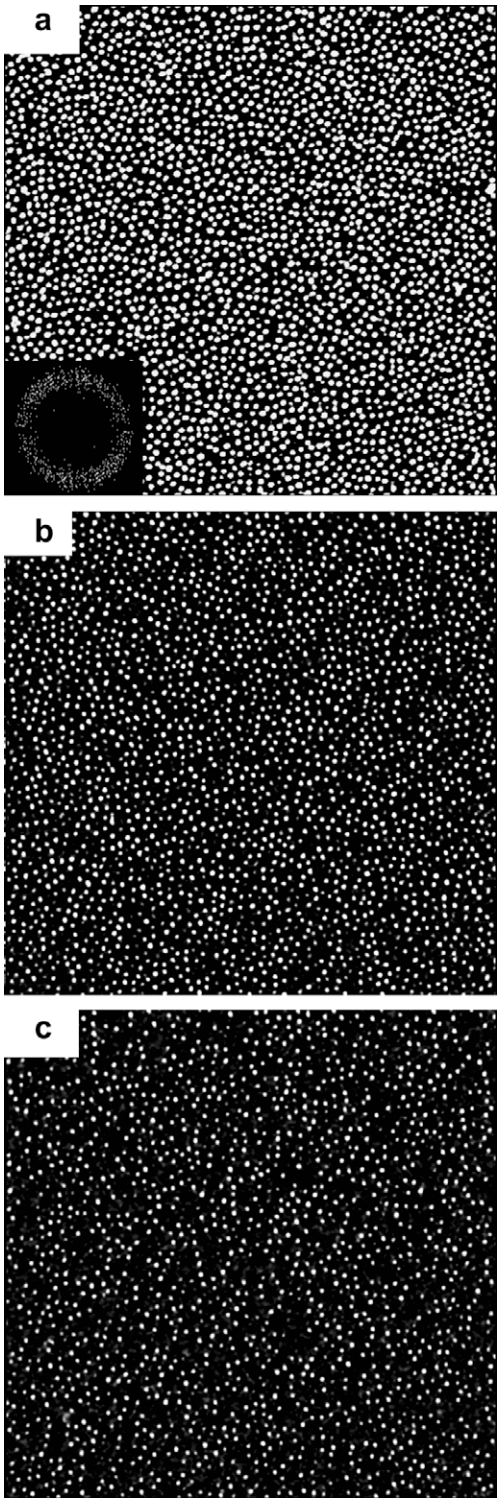

Fig. 3. $3 \times 3\ \mu m^2$ TMAFM phase images of: (a) a film of the pure acrylate radial copolymer; (b) a film of a radial copolymer–rosin resin blend with a resin content of 40 wt%; (c) a film of a radial copolymer–rosin resin blend with a resin content of 60 wt%.

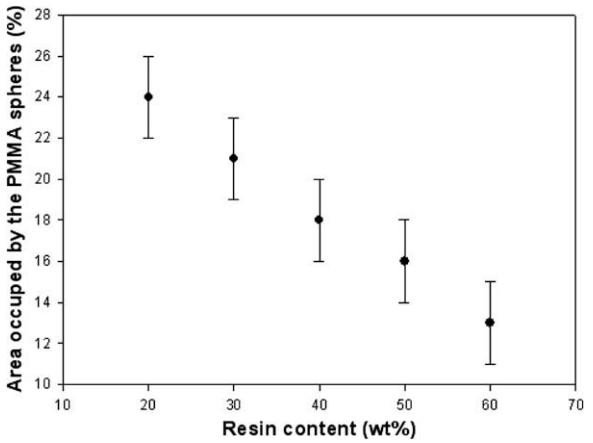

Fig. 4. Evolution of the relative surface area occupied by the PMMA spheres as a function of the resin content.

number of these defects appear to increase with the resin content. These defects are attributed to small aggregates of pure resin. Because the T_g of the resin is above room temperature (i.e., the temperature of the AFM measurements), the resin aggregates are expected to be in a glassy state, giving rise to a phase signal similar to that of the PMMA spheres. AFM images at large scale (not presented here) show that these defects are present all over the film surface. The AFM data are consistent with the DSC results, indicating that for resin contents higher than 60 wt%, there is a loss of miscibility between the elastomer part of the copolymer and the tackifying resin, due to the saturation of the elastomer matrix.

3.2. Ageing of the copolymer–resin blends

Some tackifying resins and particularly the acid rosin tackifiers used in the field of PSA are known to have a poor stability upon ageing. These resins undergo chemical changes that lead to a loss of adhesive properties. In order to improve the performance of this type of tackifiers, the resins are transformed into esters, which increase their UV resistance and heat stability. In this section, we study the effect of ageing for a blend of the radial copolymer and the rosin ester resin, at a resin content of 40 wt%, by following the surface morphology of this composition in time with AFM.

In addition to the study of the storage stability over several months at room temperature, we analyzed blends that underwent accelerated ageing by annealing. Annealing above the T_g of the blend increases the kinetics of the ageing and allows to study the process in a relatively short-time. The samples were annealed at 70 °C under atmospheric conditions during eleven days. After three, five and eleven days the samples were cooled at room temperature and analyzed with AFM. Fig. 6 shows the AFM phase images of the blends, immediately after preparation of the films (Fig. 6a), after five (Fig. 6b) and after eleven days (Fig. 6c) of ageing. Before ageing, the AFM images reveal the presence of thermoplastic PMMA spheres embedded in the elastomer matrix incorporating the resin, as

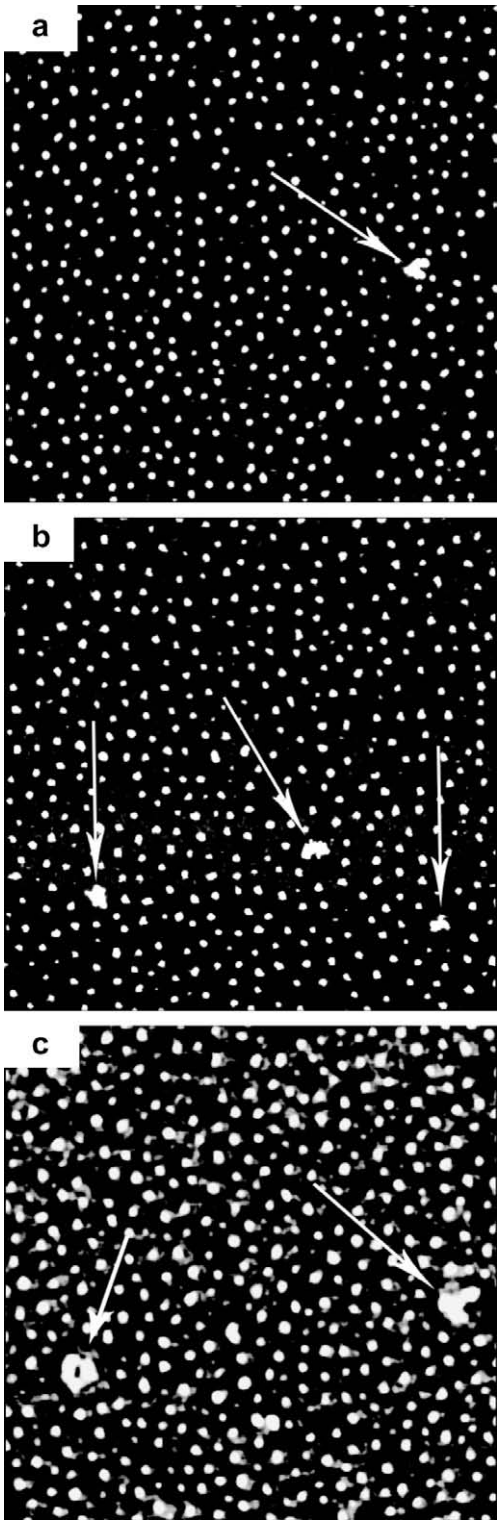

Fig. 5. TMAFM $1.5 \times 1.5\ \mu m^2$ phase images of the surface of radial copolymer–rosin resin blends. The resin contents in those blends are: (a) 70 wt%, (b) 80 wt% and (c) 90 wt%.

shown previously. After annealing for three days, no changes were observed. After five days, the morphology

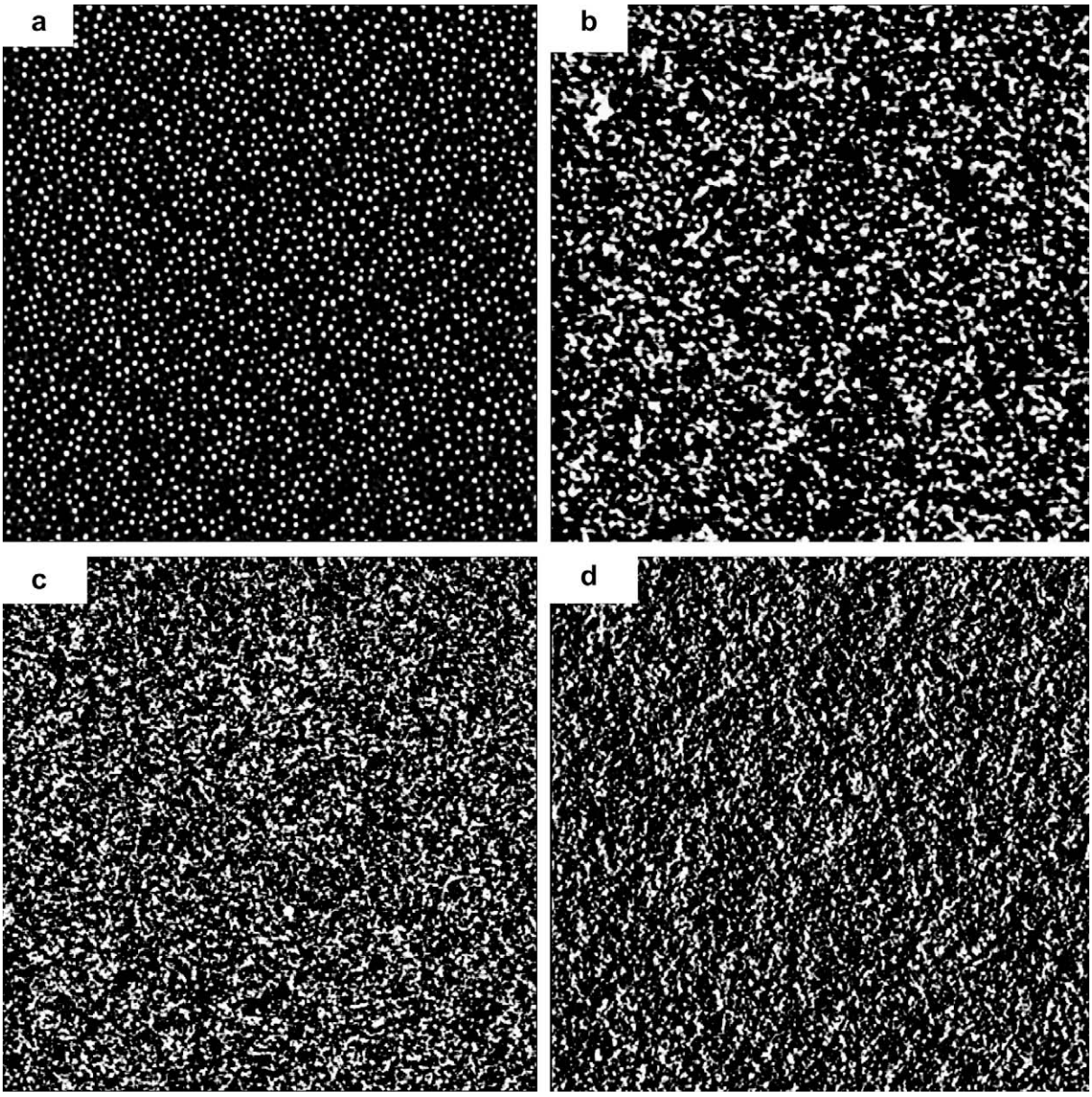

Fig. 6. TMAFM 3×3 μm^2 phase images of the surface of a blend with a resin content of 40 wt%: (a) as prepared; (b) after annealing for five days; (c) after annealing for eleven days; (d) phase image of the surface of a film of pure resin.

is modified, i.e., the regular arrangement of the PMMA spheres is lost as new bright objects, with a less defined shape, appear on the surface. This evolution is consistent with the appearance of a third phase at the surface with a T_g above room temperature. After eleven days, we observe a homogeneous surface made of a continuous arrangement of small bright features. This evolution suggests that the chemical composition of the surface changes upon annealing. We interpret these progressive changes in the morphology as a progressive migration of the pure resin to the air-film interface, which after eleven days fully covers the surface. In order to check this assumption, we have analyzed a sample of pure resin (Fig. 6d), which indeed shows a morphology very similar to that of the aged sample. For blends stored at room temperature, a similar morphological evolution takes place over a period of six to eight months. We also checked that a film of the pure copolymer, annealed at 70 °C for eleven days, undergoes no significant morphogical change.

These AFM results suggest that during the ageing of the sample there is migration of the resin towards the surface of the film. The driving mechanism behind this surface enrichment can be explained in terms of surface energetics. Using a group-additive approach (*viz.* the Van Krevelen method [20]) the surface free energy can be estimated by summing the contributions of the various structural

groups in the polymer repeat unit, as shown by the following equation:

$$\gamma = (P/V)^4$$

where γ is the surface free energy, P is the group contribution to the parachor parameters for the molecules, V is the molecular volume calculated from the molecular weight and the density of the molecule. In the present case, the copolymer has the highest surface free energy (36.1 mJ/m^2 for P(2EHA-*co*-MA) vs. 29.9 mJ/m^2 for the tackifying resin). The material evolves towards a minimum in surface free energy at the air-film interface, which leads to a preferential exposure of the tackifier with respect to P(2EHA-*co*-MA).

In order to confirm the presence of the resin layer at the surface after ageing, the samples were further analyzed with time-of-flight secondary ions mass spectrometry (TOF-SIMS). This technique is one of the most surface sensitive techniques providing molecular information for organic films/components.

Fig. 7a and b show the mass spectra of positive secondary ions (positive TOF-SIMS spectra) of samples of the pure resin and the pure radial copolymer, respectively.

The spectra show clear differences in the hydrocarbonated C2, C3 and C4 and C5 fragments for the pure resin (Fig. 7a) compared to the pure copolymer (Fig. 7b). In particular, $C_3H_3^+$, $C_4H_3^+$, $C_5H_3^+$ ions in the pure resin spectrum (marked by black arrows) are characterized by high relative intensities, these fragments corresponding typically to carbon atoms with low H/C ratio, like in the ring structure of the resin.

Fig. 8a and b show the positive mode spectrum before and after eleven days ageing of a sample containing 40 wt% resin. In the spectrum of the fresh blend (Fig. 8a), hydrocarbonated fragments of the two components are observed, confirming that both compounds are initially present at the surface of the film. After ageing, the spectrum shows the prominence of $C_3H_3^+$, $C_4H_3^+$ and $C_5H_3^+$ peaks (see black arrows on Fig. 8(b)) as observed in the pure resin spectrum (see Fig. 7a). These are clear indications of the presence of resin at the surface of the aged sample.

The samples were also analyzed in the negative ion detection mode (Table 3). These data indicate a significant evolution of the normalized intensities of the peaks upon ageing, towards the values recorded for the pure resin, confirming the trends found in the positive mode spectra.

4. Synopsis

With the aim of studying the miscibility between a tackifying resin and a symmetric four-arm radial "all-acrylate" copolymer for PSA applications, blends with increasing resin content were prepared and analyzed. The TMAFM results obtained on solution-cast films clearly show, for resin contents lower than 60 wt%, a two-phase morphology, with PMMA spheres in the elastomer matrix of poly(2EHA-*co*-MA). This result indicates that the resin is efficiently incorporated into the elastomeric part of the copolymer. This is confirmed by DSC, since all blends with resin content lower than 60 wt% show a single glass transition, intermediate between those of the pure resin and the elastomer. In the miscible range, the experimental T_g data are well described by the phenomenological Gordon–Taylor equation. After adjustment, a value $k = 0.55 \pm 0.07$ is found, which suggests a modest affinity between the elastomer matrix and the resin. For compositions with resin contents exceeding 60 wt%, TMAFM shows that the miscibility is no longer complete and part of the resin forms a separate phase due to the saturation of the elastomer matrix.

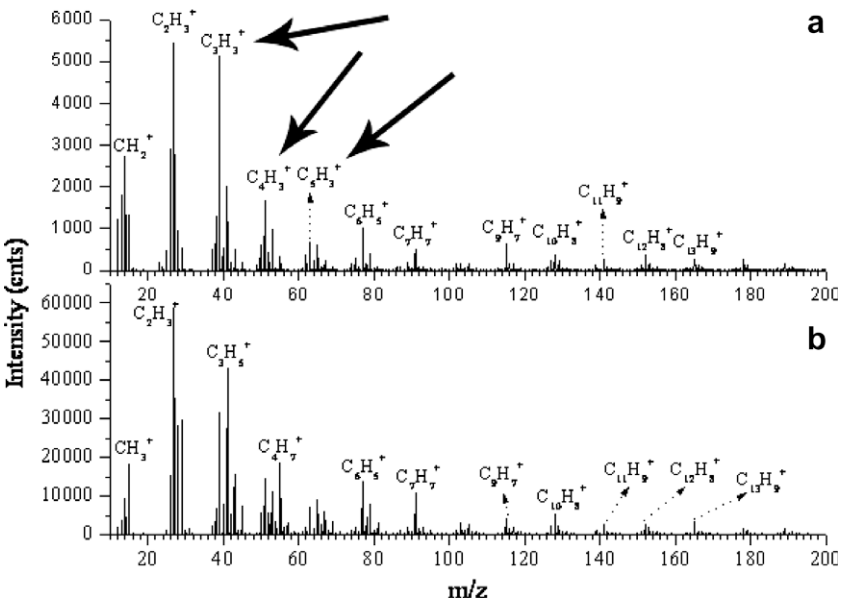

Fig. 7. Mass spectra of positive secondary ions: (a) for the pure resin; (b) for the pure radial copolymer.

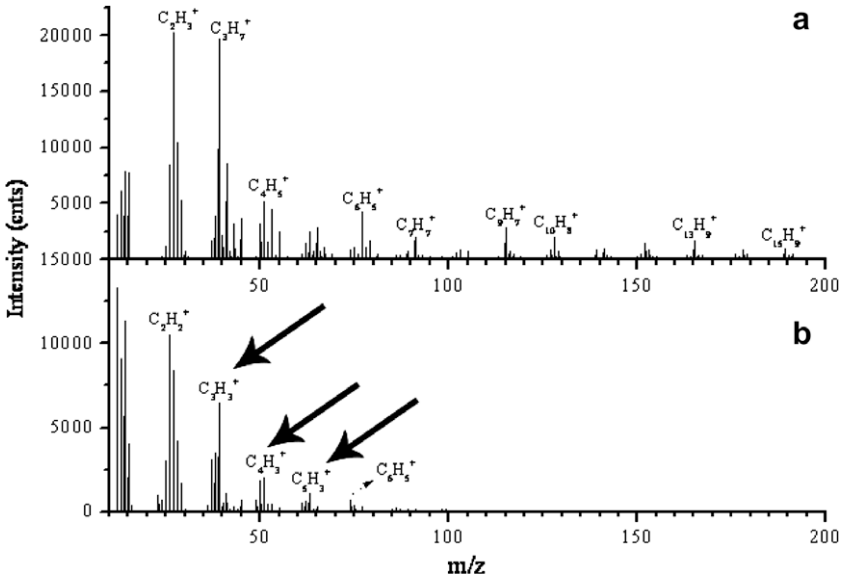

Fig. 8. Mass spectra of positive secondary ions for the blend; (a) before ageing; (b) after an ageing of eleven days at 70 °C.

Table 3
Comparison of the normalized peak intensities of the C–, CH–, O– and OH– peaks for the separated compounds and for as prepared and aged blends

	Copolymer	Resin	Blend as prepared	Blend after 6 months at RT
C^-	5107	6842	3385	7250
CH^-	9422	15,262	9889	12,235
O^-	17,223	1745	8970	2980
OH^-	8180	1309	5708	1464

The mechanical and adhesion properties of blends of the radial copolymer and the tackifying resin have been studied and are reported elsewhere [8]. The adhesive systems based on those blends give tailored peel adhesion on various substrates, together with a high cohesive strength.

In the second part of this study, we focused on the evolution of the morphology of the resin/copolymer blends upon ageing. For a resin content of 40 wt%, TMAFM and TOF-SIMS results indicate the presence of a layer of pure resin at the surface after ageing. The presence of this layer of pure resin at the surface after phase separation can be understood in terms of the difference in surface free energy between the copolymer and the resin.

Acknowledgements

Research in Mons is partly supported by the Inter-University Attraction Pole Program of the Belgian Federal Science Policy (PAI 6/27), the European Commission and the Government of the Region of Wallonia (Phasing Out-Hainaut, Materia Nova), and the Belgian National Fund for Scientific Research FNRS/FRFC. Ph.L. is Research Associate of FNRS (Belgium).

References

[1] Mallegol J, Dupont O, Keddie JL. Langmuir 2001;17:7031.
[2] Creton C. MRS Bull 2003;28:434.
[3] Benedek I. Pressure-sensitive adhesives and applications. 2nd ed. New York: Dekker Marcel; 2004.
[4] Nakajima N, Babrowicz R, Harrell ER. J Polym Sci Polym Phys Ed 1992;44:1437;
Kraus G, Rollmann KW, Gray RA. J Adhes 1979;10:221;
Brown K, Hooker JC, Creton C. Macromol Mater Eng 2002; 287:163.
[5] Schlademan JA. Handbook of pressure-sensitive adhesive technology. New York: Satas Donatas; 1989.
[6] Holden G. Understanding thermoplastic elastomers. Munich: Hanser Gardner; 2000.
[7] Mishra MK, Kobayashi S. Star and hyperbranched polymers. New York: Dekker Marcel; 1999;
Shim JS, Kennedy JP. J Polym Sci Part A Polym Chem 1999;37:815;
Puskas JE, Antony P, Kwon Y, Paulo C, Kovar M, Norton PR, Kaszas G, Altstädt V. Macromol Mater Eng 2001;286:565.
[8] Simal F, Jeusette M, Leclère Ph, Lazzaroni R, Roose P. J Adhes Sci Technol 2007;21:559.
[9] Kim H-J, Mizumachi HJ. Appl polym Sci 1995;57:175.
[10] Hayashi S, Kim H-J, Kajiyama M, Ono H, Mizumachi H, Zufu ZJ. Appl polym Sci 1999;71:651.
[11] Coulon G, Collin B, Ausserre D, Chatenay D, Russell TP. J Phys France 1990;51:2801;
Collin B, Chatenay D, Coulon G, Ausserre D, Gallot Y. Macromolecules 1992;25:1621;
van den Berg R, de Groot H, van Dijk MA, Denley DR. Polymer 1994;35:5778;
Leclère Ph, Lazzaroni R, Brédas JL, Yu JM, Dubois Ph, Jérôme R. Langmuir 1996;12:4317;
Tong JD, Leclère Ph, Doneux C, Brédas JL, Lazzaroni R, Jérôme R. Polymer 2001;42:3503.
[12] Jeusette M, Leclère Ph, Lazzaroni R, Simal F, Vaneecke J, Lardot Th, Roose P. Macromolecules 2007;40:1055.
[13] Hashimoto T, Todo A, Itoi H, Kawai H. Macromolecules 1977;10:377;
Gallot B. Adv Polym Sci 1978;29:85;
Hashimoto T, Nagatoshi K, Todo A, Hasegawa H, Kawai H. Macromolecules 1974;7:364;
Gallot B. Liquid crystalline order in polymers. In: Blumstein A, editor. New York: Academic Press; 1978. p. 233;
Todo A, Kiuno H, Miyoshi K, Hashimoto T, Kawai H. Polym Eng Sci 1977;17:587;
Hashimoto T, Shibayama M, Kawai H. Macromolecules 1980;13:1237;

Hashimoto T, Fujimura M, Kawai H. Macromolecules 1980;13:1660;
Thomas EL, Anderson DM, Henkee CS, Hoffman D. Nature 1988;334:598;
Riess G, Bahhadur P. Encyclopedia of polymer science and engineering. In: Mark HF, Bikales NM, Overberger C, Menges G, editors. New York: Wiley; 1989. p. 33;
Matthias K, Armin K, Georg K, Magerle R. Macromolecules 2000;33:5518;
Knoll A, Magerle R, Krausch G. Macromolecules 2001;34: 4159.

[14] Magonov SN, Elings V, Whangbo WH. Surf Sci Lett 1997;375:385;
Bar G, Thomman Y, Brandsch R, Cantow HJ, Whangbo MH. Langmuir 1997;13:3807;
Burnham NA, Behrend OP, Oulevey F, Gremaud G, Gallo PJ, Gourdon D, Dupas E, Kulik AJ, Pollock HM, Briggs GAD. Nanotechnology 1997;8:67;
Tong JD, Moineau G, Leclère Ph, Brédas JL, Lazzaroni R, Jérôme R. Macromolecules 2000;33:470;
Kopp-Marsaudon S, Leclère Ph, Dubourg F, Lazzaroni R, Aimé JP. Langmuir 2000;16:8432;
Leclère Ph, Dubourg F, Kopp-Marsaudon S, Brédas JL, Lazzaroni R, Aimé JP. Appl Surf Sci 2002;188:524.

[15] Gordon M, Taylor JS. J Appl Chem 1952;2:493;
Hubbell DS, Cooper SL. J Appl Poly Sci 1977;21:3035;
Koleske JV. Polymer Blends. In: Paul DR, Newman S, editors. New York: Academic Press; 1978. p. 69. vol. 2;
Galan C, Sierra CA, Gomez Fatou JM, Delgado JA. J Appl Chem 1996;62:1263.

[16] Belorgey G, Pru'dhomme RE. J Polym Sci Polym Phys Ed 1982;20:191;
Koleske JV. Polymer Blends. In: Paul DR, Newman S, editors. New York: Academic Press; 1978. p. 369. Vol. 2;
Hubbell DS, Cooper SL. J Appl Polym Sci 1995;57:175.

[17] Kim H-J, Mizumachi HJ. Appl Polym Sci 1995;58:1891.

[18] Hashimoto T, Shibayama M, Kawai H. Macromolecules 1980;13:1237;
Choi S, Lee KM, Han CD, Sota N, Hashimoto T. Macromolecules 2003;36:793.

[19] Bearing analysis, Nanoscope III software Version 5.12 r3.

[20] Van Krevelen DW. Properties of polymers. Amsterdam: Elsevier; 1990.